ACS APPLIED MATERIALS & INTERFACES

Research Article

www.acsami.org

Receptor-Based Detection of 2,4-Dinitrotoluene Using Modified Three-Dimensionally Ordered Macroporous Carbon Electrodes

Melissa A. Fierke,† Eric J. Olson, Philippe Bühlmann,* and Andreas Stein*

Department of Chemistry, University of Minnesota, 207 Pleasant Street SE, Minneapolis, Minnesota 55455, United States

Supporting Information

ABSTRACT: Detection of explosives, such as 2,4,6-trinitrotoluene (TNT), is becoming increasingly important. Here, 2,4-dinitrotoluene (DNT, a common analogue of TNT) is detected electrochemically. A receptor based electrode for the detection of DNT was prepared by modifying the surface of the walls of three-dimensionally ordered macroporous (3DOM) carbon. Nitrophenyl groups were first attached by the electrochemical reduction of 4-nitrobenzenediazonium ions, followed by potentiostatic reduction to aminophenyl groups. Chemical functionalization reactions were then performed to synthesize the receptor, which contains two urea groups, and a terminal primary amine. Detection of DNT using cyclic voltammetry was impeded by a large background current that resulted from the capacitance of 3DOM carbon. Detection by square wave voltammetry eliminated the background current and improved the detection limit. Unfunctionalized 3DOM carbon electrodes showed no response to DNT, whereas the receptor-modified electrodes responded to DNT with a detection limit of 10 μM. Detection of DNT was possible even in the presence of interferents such as nitrobenzene.

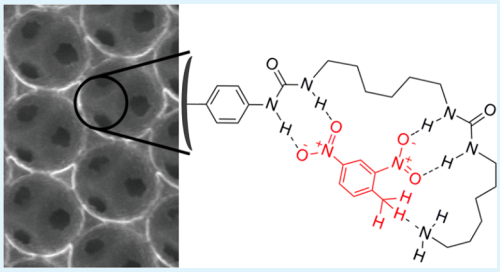

KEYWORDS: *three-dimensionally ordered macroporous carbon, dinitrotoluene, voltammetry, receptor, explosive, functionalization*

INTRODUCTION

The detection of explosives, including 2,4,6-trinitrotoluene (TNT), is an important analytical problem of relevance for the prevention of terrorism and for the detection of military explosives (including leftover landmines) and environmental hazards from improperly disposed explosives.[1] Rather than attempting to detect TNT directly, researchers often focus on detecting 2,4-dinitrotoluene (DNT).[2−4] DNT, which is a common impurity in TNT-based explosives,[5] exhibits a higher volatility than TNT, allowing for considerably more sensitive detection. In fact, DNT is the component of TNT-based explosives that canines are able to detect with very good sensitivity.[5,6]

Many methods of DNT detection have been reported, including photoluminescence and fluorescence quenching,[7,8] detection of reduction or degradation products,[9−11] vapor adsorption on a modified microcantilever,[12] electronic noses and sniffers,[3,13] electrochemical impedance detection,[14] and detection by combining capillary electrophoresis and electrochemical detection with a porous-carbon-modified electrode.[15] For the purpose of miniaturization, electrochemical detectors are attractive for sensing explosives.[14,16−19] Electrode miniaturization offers many benefits, including reduced cost, which enhances the feasibility of creating sensor networks, and greater portability. Moreover, the adaptation of an electrochemical sensor to detect explosive compounds is rather straightforward, as their structures make them inherently redox active. A common theme in most published electrochemical sensors for DNT, however, is that their selectivity is determined largely by the redox potential of the analyte. The addition of a supramolecular receptor that specifically binds the analyte has the potential for greatly improving both the selectivity and sensitivity of detection.[20] In fact, molecular recognition schemes have previously been developed for the electrochemical detection of the related compound TNT.[21,22]

In this work, a receptor-modified, three-dimensionally ordered macroporous (3DOM) carbon electrode was used to detect DNT electrochemically. The use of porous electrodes, including carbon electrodes, for electroanalytical applications has recently been reviewed.[23,24] 3DOM carbon, a conductive material composed of glassy carbon walls that surround an ordered array of interconnected pores (Figure 1), is a particularly attractive electrode material due to its highly accessible and relatively large surface.[25,26] For sensing applications, 3DOM carbon has previously been used as an electrode for solid-state ion-selective and reference electrodes, and extremely low detection limits and very small EMF drifts were achieved.[27−30] As prepared, the walls of 3DOM carbon do not contain many functional groups,[27] and further functionalization is required to attach receptor molecules. The functionalization scheme used to modify the walls of the pores in 3DOM carbon is shown in Figure 1. After functionalization with nitrophenyl groups by diazonium reduction, the nitro groups are reduced to amino groups, which provide an aminophenyl functionalized surface that can be chemically modified by many different methods.[31] Here, 1,6-

Received: June 19, 2012
Accepted: August 20, 2012
Published: August 20, 2012

   dx.doi.org/10.1021/am301108a | ACS Appl. Mater. Interfaces 2012, 4, 4731−4739

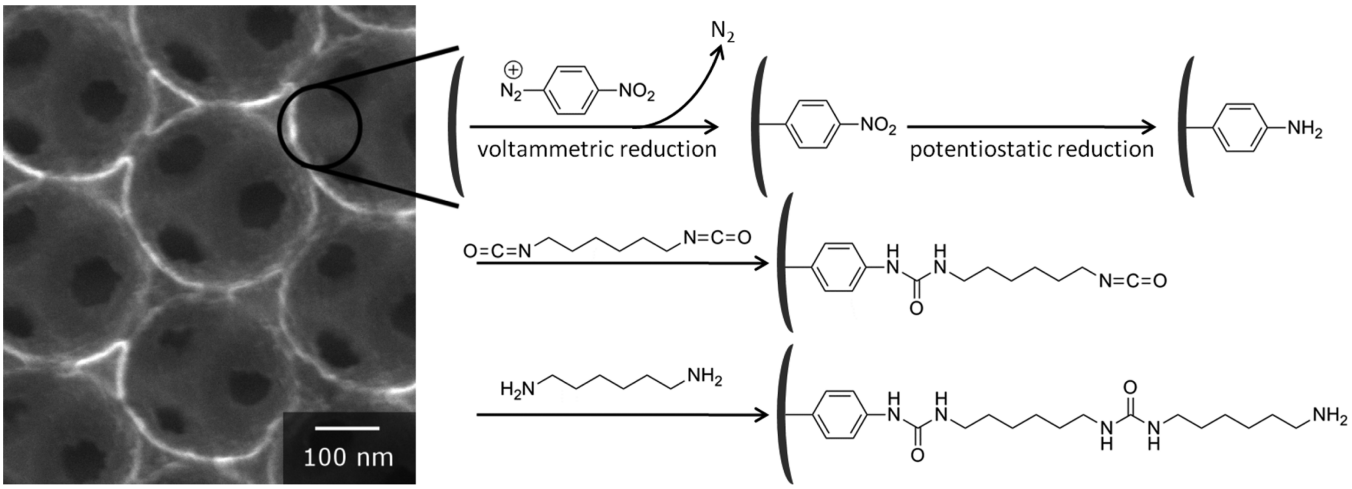

Figure 1. Scheme for functionalization of 3DOM carbon (left) to produce receptor-modified electrodes through electrochemical and chemical modification steps.

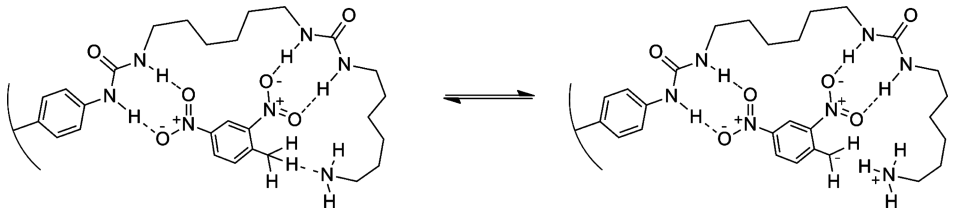

Figure 2. Anticipated interaction between DNT and the receptor on the surface of the 3DOM carbon.

diisocyanatohexane was reacted with the aminophenyl groups, followed by reaction with 1,6-hexanediamine to give a receptor with two urea groups and a terminal aliphatic amine to interact with DNT.

This receptor molecule was chosen on the basis of previous work, which conclusively showed that in DMSO solutions, the methyl group of DNT is deprotonated by bases such as amines.[32] In the case of the receptor that we designed herein, we expected that DNT would be deprotonated by the terminal amino group of the receptor. The resulting deprotonated DNT would exhibit partial anionic character at each nitro group due to resonance. Because urea moieties are well-known to be good hydrogen bond donors,[31] they are expected to interact rather strongly with the electron-rich nitro groups. By stabilizing the anionic nature of the nitro groups of deprotonated DNT, binding of DNT with the developed receptor would likely lower the pK_a of DNT and therefore further stabilize the DNT:receptor complex. The anticipated geometry of the DNT:receptor interaction is shown in Figure 2.

In this article, we describe the synthesis and characterization of the receptor-modified 3DOM carbon electrodes and evaluate their performance as DNT sensors in cyclic voltammetry (CV) and square wave voltammetry (SWV) experiments. By SWV, a detection limit of 10 μM was established.

EXPERIMENTAL SECTION

Materials. All reagents were of the highest commercially available purity. Resorcinol, 4-nitrobenzenediazonium tetrafluoroborate, 1,6-diisocyanatohexane, 1,6-hexanediamine, boron trichloride (1.0 M in heptane), *t*-butyl lithium (1.7 M in pentane), 2,4-dinitrotoluene, and benzotrifluoride (α,α,α-trifluorotoluene) were from Sigma-Aldrich (St. Louis, MO), tetrabutylammonium chloride and tetrabutylammonium tetrafluoroborate were from Fluka (Milwaukee, WI), formaldehyde (37% in H_2O) was from Fisher Scientific (Pittsburgh, PA), 1-bromo-3,5-bis(trifluoromethyl)benzene was from SynQuest Laboratories (Alachua, FL), unplasticized PVC sheets were from Goodfellow (Oakdale, PA), and Ni mesh was a gift from Dexmet (Branford, CT). All chemicals were used as received.

Synthesis of 3DOM Carbon Electrodes. 3DOM carbon monoliths were synthesized as previously described.[28] In brief, colloidal crystal templates composed of 425 nm poly(methyl methacrylate) (PMMA) spheres were infiltrated with a base-catalyzed resorcinol-formaldehyde prepolymer. After heating at 85 °C for 3 days to cross-link the polymer, the infiltrated templates were pyrolyzed at 900 °C for 2 h with a ramp rate of 5 °C min^{-1} under flowing nitrogen to remove the PMMA template and carbonize the cross-linked resorcinol−formaldehyde polymer. After polishing the porous carbon with sandpaper to produce monoliths with typical dimensions of 5 mm × 5 mm × 0.5 mm, the monoliths were affixed to a nickel mesh current collector using resorcinol−formaldehyde carbon precursor that had been heated for ca. 20 min, followed by curing at 85 °C overnight to produce 3DOM carbon electrodes.

Nitrophenyl Functionalization of 3DOM Carbon Electrodes. Nitrophenyl functional groups on the walls of the pores in 3DOM carbon were produced electrochemically by an adapted version of a previously published method.[33,34] Functionalization of the porous electrode requires a high concentration of the diazonium salt because diffusion through the pores is not fast enough to allow for replenishment of the solution in the pores from the bulk solution. A nonaqueous reference electrode and a platinum wire counter electrode were placed in a 25 mL round-bottom flask. Approximately 2 mL of the functionalization solution (an acetonitrile solution containing 0.1 M tetrabutylammonium tetrafluoroborate electrolyte and saturated with 4-nitrobenzenediazonium tetrafluoroborate) was added. After purging the solution with argon for 10 min, the 3DOM carbon electrode was submerged in the solution. Bubbles immediately emerged from the carbon electrode, indicating wetting of the porous carbon by the electrolyte solution. The functionalization was carried out using cyclic voltammetry, with a window of +0.8 to −1.7 V vs Ag/10 mM $AgNO_3$ (CH_3CN) and a sweep rate of 10 mV s^{-1} for 2−4 cycles (until consecutive cycles overlapped well). After functionaliza-

tion, the electrode was thoroughly cleaned by soaking in fresh acetonitrile several times.

Aminophenyl Functionalization of 3DOM Carbon Electrodes. The nitrophenyl functional groups on the walls of the 3DOM carbon were electrochemically reduced to aminophenyl functional groups. The modified electrode was placed in an aqueous 0.1 M phosphate buffer ($NaH_2PO_4{\cdot}H_2O/Na_2HPO_4{\cdot}7H_2O$) solution (10 v/v % ethanol was added to facilitate wetting, pH 7.1) with a double-junction Ag/AgCl reference electrode and a platinum wire counter electrode. A constant potential of −1.4 V versus the reference electrode was applied for 2 h. The electrodes were then cleaned by soaking in fresh water/ethanol solution several times.

Reaction with 1,6-Diisocyanatohexane. The aminophenyl-modified electrodes were reacted with 1,6-diisocyanatohexane, forming a urea group between an isocyanate functionality and the $-NH_2$ of the aminophenyl on the surface of the carbon electrode. This process leaves a free isocyanate group on the end of the receptor. An aminophenyl functionalized electrode was placed in a small flask. Approximately 4 mL neat 1,6-diisocyanatohexane was added to the flask, completely covering the carbon component of the electrode. The flask was attached to a water-cooled condenser and heated in an oil bath at 120 °C for 24 h. The electrode was then removed from the flask and cleaned by soaking in fresh toluene several times.

Reaction with 1,6-Hexanediamine. A second urea group and a terminal amino group were formed by reacting the isocyanate-functionalized electrodes with 1,6-hexanediamine, forming the complete receptor. An isocyanate-functionalized electrode was placed in a small flask. Approximately 4 mL of a 10 w/w% solution of 1,6-hexanediamine in toluene was added. The flask was attached to a water-cooled condenser and heated in an oil bath at 120 °C for 24 h. The electrode was then removed from the flask and cleaned by soaking in fresh toluene several times.

Electrode Encasement. Before use, fully modified electrodes were encased in unplasticized poly(vinyl chloride) (PVC) to provide mechanical stability and electrical insulation. PVC sheets sealed with commercial PVC adhesive were used to encase the entire electrode, except for the functionalized 3DOM carbon and a small portion of the Ni mesh on the opposite end of the electrode construct (to allow for electrical contact).

Synthesis of NBu_4BArF_{24}. After optimization, a solvent/electrolyte combination of benzotrifluoride with tetrabutylammonium tetrakis[3,5-bis(trifluoromethyl)phenyl]borate (NBu_4BArF_{24}) was selected (Figure S1 in the Supporting Information). Benzotrifluoride was chosen because it does not interact with the receptor on the carbon surface, which would prevent detection of DNT. It also does not dissolve or soften the electrode encasement material. NBu_4BArF_{24} is soluble to 100 mM in benzotrifluoride and sufficiently lowers the resistance to allow electrochemical experiments to be carried out.

Sodium tetrakis[3,5-bis(trifluoromethyl)phenyl]borate was prepared as follows by adaptation of a previously described procedure for the synthesis of sodium tetrakis[3,5-bis(perfluorohexyl)phenyl]-borate.[35] All synthetic steps were carried out in an argon atmosphere, unless otherwise noted. A 1.7 M solution of *t*-butyl lithium (76 mL, 130 mmol, 9.2 equiv) was added over 30 min by addition funnel to a stirred solution of 1-bromo-3,5-bis(trifluoromethyl)benzene (10 mL, 56 mmol, 4.7 equiv) chilled to −76 °C. After the solution was allowed to stir for 30 min, a 1.0 M BCl_3 solution (12 mL, 12 mmol, 1 equiv) was added dropwise by syringe over 10 min. Upon complete addition of the BCl_3 solution, the reaction mixture was warmed slowly to room temperature and stirred vigorously for an additional 2 h. The crude mixture was then slowly poured into 100 mL of NaCl-saturated water (the remaining steps are not air-sensitive) and vigorously mixed. This mixture was then extracted with diethyl ether (3 × 100 mL). The organic layers were combined, dried with anhydrous $MgSO_4$, and rotary evaporated to yield a pale yellow oil. This oil was dried at 100 °C under vacuum to produce a tan-yellow solid. The product was recrystallized 3 times from benzotrifluoride by addition of hexane to produce high purity $NaBArF_{24}$ as a fine white powder (40% yield). ^{1}H NMR (300 MHz, acetone-d_6, δ): 7.69 (s, *p*-Ar*H*, 4H), 7.81 (s, *o*-Ar*H*, 8H). These NMR shifts are in good agreement with previously published results for this compound.[36−38]

NBu_4BArF_{24} was synthesized by metathesis from tetrabutylammonium chloride and sodium tetrakis[3,5-bis(trifluoromethyl)phenyl]-borate: 8.0 g of sodium tetrakis[3,5-bis(trifluoromethyl)phenyl]borate and 1.0 g of tetrabutylammonium chloride were added to a separatory funnel containing 300 mL water and 300 mL benzotrifluoride. The mixture was shaken until all of the salt dissolved. The organic layer was collected, washed three times with 300 mL water, dried with $MgSO_4$, and filtered. The solvent was removed by rotary evaporation and further drying under vacuum at 75 °C for 48 h, yielding NBu_4BArF_{24} as a pale yellow, wax-like material in quantitative yield. ^{1}H NMR (300 MHz, acetone-d_6, δ): 1.00 (t, J_{HH} = 7.2 Hz, $-CH_3$, 12H), 1.46 (m, $-CH_2CH_3$, 8H), 1.86 (m, NCH_2CH_2-, 8H), 3.48 (m, NCH_2-, 8H), 7.69 (s, *p*-Ar*H*, 4H), 7.80 (s, *o*-Ar*H*, 8H).

Characterization. The nitrophenyl and aminophenyl functionalized 3DOM carbon samples were characterized by X-ray photoelectron spectroscopy (XPS). After removal from the Ni mesh, the carbon samples were mounted on the sample stage using conductive carbon sticky tape. XPS measurements were carried out on a Surface Science SSX-100 instrument with an Al anode (Kα X-rays at 1486.66 eV) operated at 10 kV and 20 mA. Measurements were performed at room temperature, with a pressure below 1×10^{-8} Torr in the analysis chamber. FTIR spectra for all functionalized 3DOM carbon samples were obtained using KBr pellets in a Nicolet Magna-IR 760 spectrometer.

Electrochemical Measurements. All cyclic voltammetry measurements were performed at room temperature with a CHI600C Potentiostat (CH Instruments, Austin, TX) while square wave voltammetry experiments were performed with a Cypress Systems 1090 Potentiostat (Cypress Systems, Lawrence, KS). All electrochemical experiments utilized a three-electrode setup with a 3DOM carbon electrode as the working electrode, a Ag/10 mM $AgNO_3$ acetonitrile reference electrode (CH Instruments) and a 0.25 mm Pt wire coil (99.998%, Alfa Aesar, Ward Hill, MA) as the auxiliary electrode. Each sample solution contained 100 mM NBu_4BArF_{24} in benzotrifluoride; DNT was introduced to the electrolyte solution by addition of stock solutions. Each sample was thoroughly purged of oxygen by bubbling high-purity argon for 20 min prior to each measurement. An argon atmosphere was maintained over the solution during measurements. Scan rates and window sizes for each experiment are indicated below. For CV experiments, multiple cycles were performed, but only cycle 2 is shown for clarity. Electrodes were evacuated using a vacuum pump for at least one hour between uses to allow for better wetting with the solution for the next experiment. SWV experiments were performed as usual, i.e., the electrode was kept at an initial potential followed by a decrease of the applied potential by the SW amplitude (often referred to as the forward pulse), and then to the original potential minus the SW amplitude (often referred to as the reverse pulse). The applied potential for the forward and reverse pulse was then decreased by 5 mV for each subsequent cycle until the desired end potential was reached. Each potential was kept constant for half of the time period, referred to below as pulse length. The SW voltammogram was obtained by plotting the differences between the currents at the end of each forward pulse and the following reverse pulse.

RESULTS AND DISCUSSION

3DOM Carbon Electrode Functionalization. 3DOM carbon electrodes were first electrochemically functionalized with nitrophenyl groups by voltammetric reduction of 4-nitrobenzenediazonium (Figure 3). In the first cycle, a large, irreversible peak at −0.5 V was observed, and is attributed to the reduction of 4-nitrobenzenediazonium to its aromatic radical,[33,34] which then bonds with the surface of the carbon pore walls. In the subsequent voltammetric cycles, the peak decreased until it was no longer present in cycle 4, indicating maximum coverage of the 3DOM C surface with nitrophenyl

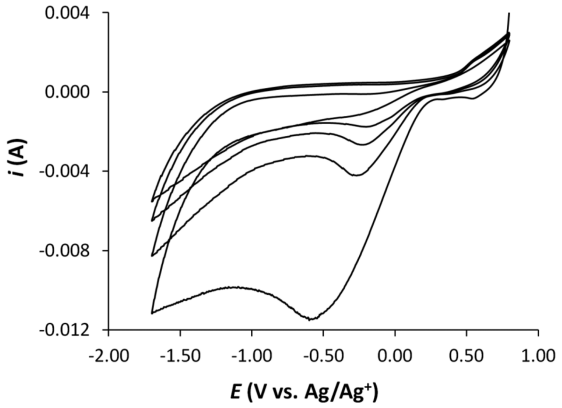

Figure 3. Voltammetric functionalization of a 3DOM carbon electrode with a saturated acetonitrile solution of 4-nitrobenzenediazonium tetrafluoroborate (with 0.1 M tetrabutylammonium tetrafluoroborate as the electrolyte), producing nitrophenyl functionalization on the pore walls of the carbon. A scan window of +0.8 to −1.7 V and a scan rate of 10 mV s^{-1} were used.

groups. The number of cycles required to complete the reaction depended on the surface area of the 3DOM carbon monolith.

The nitro groups on the nitrophenyl modified electrodes were then potentiostatically reduced at −1.4 V in an aqueous phosphate buffer solution. XPS was carried out on reduced and nonreduced samples to verify the reduction of nitro groups to amino groups (Figure 4). The bonding environment of nitrogen atoms can be determined by examining the N_{1s} region. Nitrogen atoms in nitro groups produce a peak at 406 eV whereas nitrogen atoms in amino groups produce a peak at 400 eV.[33] The XPS spectrum of nitrophenyl functionalized carbon exhibited peaks at both of these positions (Figure 4A). The peak at 406 eV indicates that the walls of the 3DOM carbon were successfully modified with nitrophenyl groups. The additional peak at 400 eV after grafting of nitrophenyl groups has been observed previously.[39−44] Although it suggests the presence of reduced nitrophenyl groups on the surface of the carbon, the peak likely indicates that azo groups were present on the functionalized surface,[41,42] possibly as part of a multilayer film.[44,45]

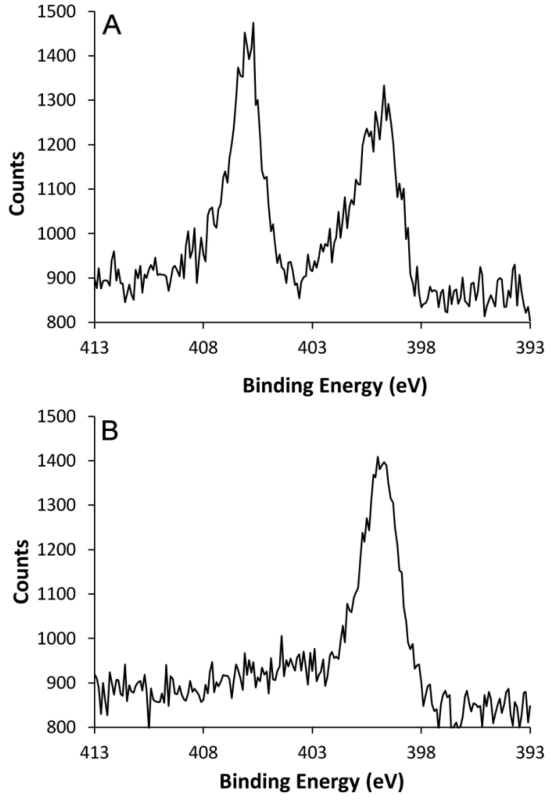

Figure 4. XPS spectra of the N_{1s} region of (A) nitrophenyl and (B) aminophenyl functionalized carbon.

After potentiostatic reduction of the nitrophenyl modified electrode in an aqueous buffer, only one peak at 400 eV was observed in the XPS spectrum (Figure 4B), consistent with the presence of aminophenyl functional groups.[41,43,46]

After additional chemical functionalization to complete the synthesis of the receptor, FTIR spectroscopy was performed to confirm the presence of the desired functional groups (Figure 5). A low concentration of sample in the KBr pellets was required, as carbon absorbs strongly in the infrared.[47] However, the concentration was sufficient to achieve spectra with peaks characteristic of the functional groups attached to the surface of the 3DOM carbon walls. A sample of unfunctionalized 3DOM carbon was also characterized for comparison. The large peak at ∼3400 cm^{-1} in each spectrum is due to water adsorbed on the surface of the carbon. In the unfunctionalized sample (Figure 5A), the peak at 1575 cm^{-1} is assigned to the skeletal structure of the 3DOM carbon.[48,49] The peaks at 1200 cm^{-1} and 1135 cm^{-1} result from C−O stretching in the oxygen-containing functional groups that exist on the as-made carbon.[27,50,51]

After voltammetric functionalization with nitrophenyl groups and potentiostatic reduction to aminophenyl groups, new peaks appear in the FTIR spectrum (Figure 5B). The peak at 1514 cm^{-1} is due to the aromatic C−C stretch of the aminophenyl group.[52] The expected amine N−H stretch at ∼3400 cm^{-1} overlaps with the water peak. However, the NH_2 deformation peak at 1597 cm^{-1} is present.[52,53]

Reaction of the aminophenyl functionalized carbon with 1,6-diisocyanatohexane forms a urea group between the amine and an isocyanate group. The attached functionality also contains an aliphatic chain and a terminal isocyanate group. As with the aminophenyl functionalized sample, the FTIR spectrum of diisocyanate funtionalized 3DOM carbon (Figure 5C) exhibits an aromatic C−C stretch at 1514 cm^{-1}. The aliphatic portion of the functionality is confirmed by the C−H stretching peaks at 2920 and 2850 cm^{-1}. The C═O stretch of the urea group appears at 1668 cm^{-1}, and the NH_2 deformation peak of the urea group is at 1615 cm^{-1}.[52] It is conceivable that some 1,6-diisocyanatohexane molecules do not react to give an attached molecule with the linear structure shown in Panel C of Figure 5 but instead form a bridge between two aminophenyl groups.

The further reaction of the diisocyanate functionalized 3DOM carbon with 1,6-hexanediamine forms another urea group with the remaining isocyanate group, adding another aliphatic chain, and leaving a free primary amine. As expected, the FTIR spectrum for the diamine functionalized sample (Figure 5D) contains the aromatic C−C stretch at 1514 cm^{-1}, C−H stretches from the aliphatic chains at 2920 and 2850 cm^{-1}, the C═O stretch of the urea group at 1668 cm^{-1}, and the NH deformation peak of the urea group at 1615 cm^{-1}.[52] No peaks for the free primary amine are visible. The peak at ∼3400 cm^{-1} is overlapped by the adsorbed water peak.

Voltammetric Response to DNT. Initial characterization of the functionalized electrodes was performed with cyclic voltammetry to allow direct comparison to previously published

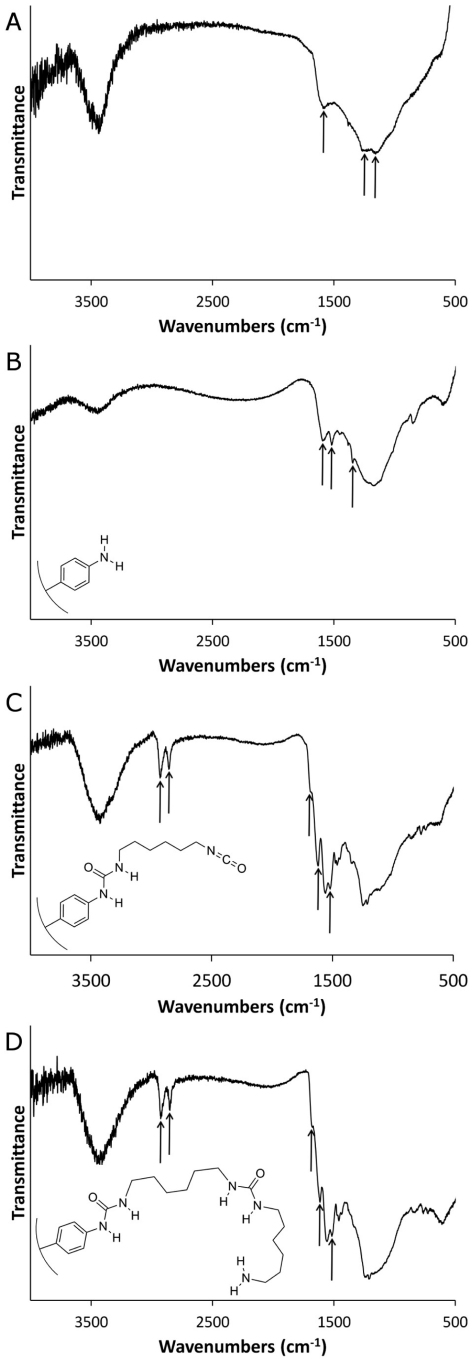

Figure 5. FTIR spectra of (A) unfunctionalized 3DOM carbon, and (B) aminophenyl-, (C) isocyanate-, and (D) diamine-functionalized 3DOM carbon. Insets show schematically the carbon surface and the surface functionalities. The arrows point to the peaks described in the text.

CV methods for the detection of nitroaromatic molecules.[18,54] In one such study, a detection limit of 5 ppb for 2,4-DNT was achieved using cyclic voltammetry with a glassy carbon electrode modified with multiwalled carbon nanotubes. Several other nitroaromatic compounds could also be detected at higher detection limits.[55] A similar method was used to detect TNT and DNT with glassy carbon electrodes modified with ordered mesoporous carbon using adsorptive stripping voltammetry to achieve a detection limit of 1 ppb for 2,4-DNT.[56] Mesoporous silica (MCM-41) modified electrodes have also been used to detect 2,4-DNT and other nitroaromatic compounds.[57]

Before testing the fully functionalized 3DOM carbon electrodes for their response to DNT, a gold electrode was used to investigate the reduction behavior of DNT in electrolyte solution (NBu_4BArF_{24} in benzotrifluoride) (Figure 6). After addition of 0.3 mM DNT to the electrolyte solution,

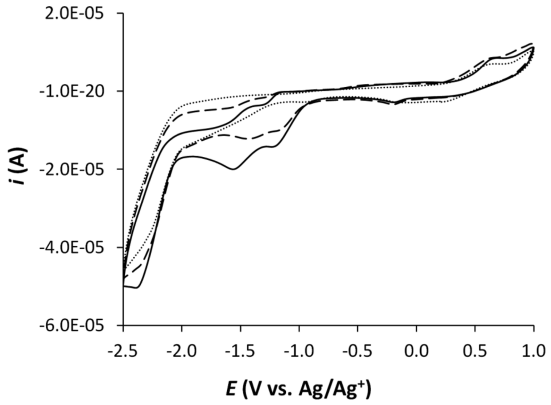

Figure 6. CV characterization of a gold electrode in benzotrifluoride/100 mM NBu_4BArF_{24} with varied DNT concentrations (····· 0 mM, – – – 0.3 mM, and — 0.6 mM). A scan window of −2.5 to +1 V starting at +0.2 V was used, with a scan rate of 100 $mV{\cdot}s^{-1}$. Only cycle 2 is shown.

two reduction waves appeared at −1.2 and −1.5 V vs Ag/Ag^+. As expected, the magnitude of the peaks increased as the concentration of DNT in the solution increased to 0.6 mM. The presence of two reduction waves for DNT is consistent with previous work for nitrobenzene and 1,4-dinitrobenzene in acetonitrile.[58] In this previous work, a single reduction wave at −1.505 V vs Ag/Ag^+ was observed for nitrobenzene while two reduction waves at −1.078 and −1.278 V vs Ag/Ag^+ were observed for 1,4-dinitrobenzene. On the basis of the behavior of the gold microelectrode, reduction peak(s) for DNT were expected at approximately −1.5 V for the modified 3DOM carbon electrode.

When obtaining voltammograms of the fully modified 3DOM carbon electrodes, a wide scan window (+2 to −5 V) was used to ensure that all possible peaks were observed. A slower scan rate (10 $mV{\cdot}s^{-1}$) was also required to obtain a well-shaped voltammogram. DNT concentrations of 0, 0.4, and 0.8 mM DNT were tested (Figure 7A). After addition of 0.4 mM DNT, the current increased beginning at −1.0 V as compared to the background scan with 0 mM DNT. After addition of an additional 0.4 mM DNT (for a total of 0.8 mM DNT), a well-defined peak at about −1.7 V was observed. The magnitude of the peak continued to increase as the concentration of DNT in the solution was increased (data not shown).

Response of Unfunctionalized 3DOM Carbon. The response of unfunctionalized 3DOM carbon electrodes to DNT was tested in an identical manner to the functionalized electrodes (Figure 7B). The first noticeable difference between the voltammograms of unfunctionalized and functionalized carbon is the total current, which is much larger for the unfunctionalized carbon. The electrochemical functionalization process blocks some micropores in the functionalized electrodes, lowering the surface area compared to the unfunctionalized electrodes. A baseline voltammogram (0 mM DNT) overlaps very well with voltammograms in solutions containing 0.2 and

dx.doi.org/10.1021/am301108a | ACS Appl. Mater. Interfaces 2012, 4, 4731−4739

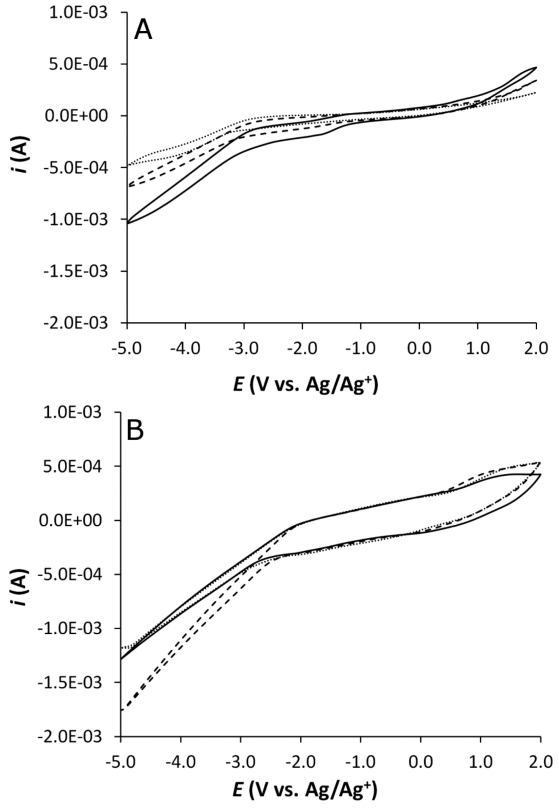

Figure 7. (A) CV characterization of a fully functionalized 3DOM carbon electrode in benzotrifluoride/100 mM NBu_4BArF_{24} with varied DNT concentrations (····· 0 mM, – – – – 0.4 mM, and — 0.8 mM). (B) CV characterization of an unfunctionalized 3DOM carbon electrode in benzotrifluoride/100 mM NBu_4BArF_{24} with varied DNT concentrations (····· 0 mM, – – – – 0.2 mM, and — 0.6 mM). A scan window of −5 to 2 V starting at −0.4 V was used, with a scan rate of 10 mV·s^{-1}; for each experiment, only the 2nd cycle is shown.

0.6 mM DNT, indicating a lack of response of unfunctionalized 3DOM carbon electrodes to DNT. Detection of DNT occurred only after modification of the electrode, giving selective detection of DNT with this method. The system also did not respond to the common interferents phenol and nitrobenzene (see the Supporting Information).

Although cyclic voltammetry demonstrates a response of the fully functionalized 3DOM carbon electrodes to DNT, the peak sizes are quite small. The rather poor limit of detection is not due to poor sensitivity of the technique, but rather an inability to distinguish between Faradaic and capacitive currents.[59] Because of the large capacitance of 3DOM C in an electrolyte solution,[27] the electrodes developed here are especially vulnerable to this limitation of cyclic voltammetry. Various techniques have been developed that allow for elimination of capacitive currents.[60] Of these, square wave voltammetry (SWV) is an extremely attractive technique for determination of analytes with electrodes that have rather large capacitance.[59,60] SWV has been well-characterized in the literature.[61−64] In addition, it has been used in recent attempts to detect explosive compounds,[65,66] including a study utilizing carbon fiber electrodes.[18] Square wave voltammetry was used here to investigate the response of the electrodes to DNT while eliminating the signal from the capacitance of the electrode, with the goal of obtaining a lower detection limit.

Optimization of SWV Parameters. When using square wave voltammetry, the optimal square wave (SW) pulse length must first be determined. To this extent, a solution of 1 mM DNT was interrogated with varying pulse lengths. As shown in Figure 8, the peak current observed for the reduction of DNT

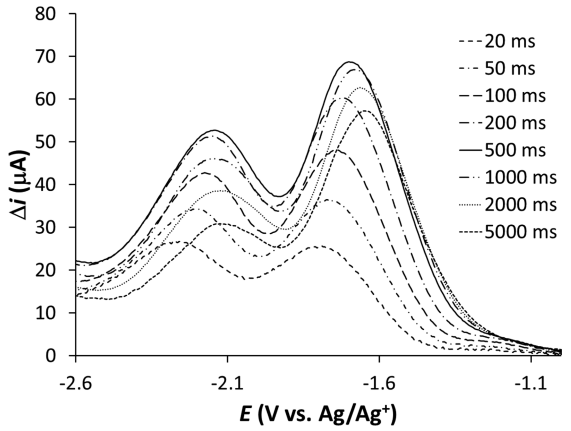

Figure 8. Square wave voltammograms of 1 mM DNT at a functionalized 3DOM carbon electrode in benzotrifluoride/100 mM NBu_4BArF_{24} with varied square wave pulse lengths (20−5000 ms). T = 20 °C, SW amplitude = 101 mV, potential step = 5 mV.

increased with increasing pulse length up to 500 ms, where the current began decreasing with subsequent increases in pulse length. This observation may be explained as follows: at rather short pulse lengths, the current observed is largely capacitive,[67] whereas at rather long lengths, the DNT contained in the pores of the 3DOM carbon is largely consumed and the current observed results solely from diffusion to the surface of the electrode. Consequently, a 500 ms pulse length was used for all subsequent experiments.

When using SWV, it is also necessary to determine the optimal SW amplitude. Shown in Figure 9 is the dependence of the peak current upon the SW amplitude.

As observed in Figure 9, the peak current for the reduction of DNT increased with increasing SW amplitude. Also, as the SW amplitude increased, there was a marked decrease in the resolution between the two reductions observed for DNT. These effects are consistent with the theory of SWV response.[59]

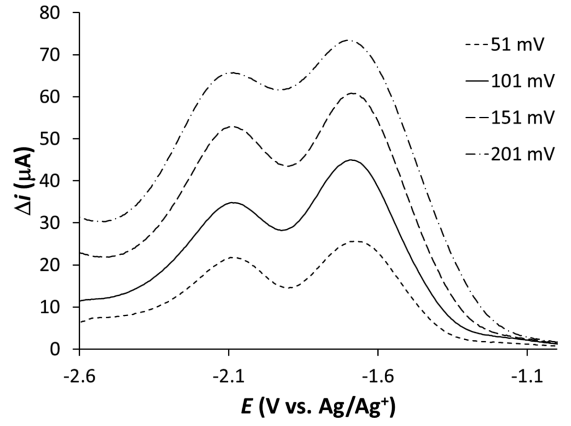

Figure 9. Square wave voltammograms of 1 mM DNT at a functionalized 3DOM carbon electrode in benzotrifluoride/100 mM NBu_4BArF_{24} with varied square wave amplitude (51−201 mV). T = 20 °C, SW pulse length = 500 ms, potential step = 5 mV.

While it may seem advantageous to choose an extremely large SW amplitude, the corresponding loss in resolution is undesirable for analytical applications. Therefore, an amplitude of 101 mV was chosen as a compromise between current sensitivity and resolution for all subsequent experiments.

Determination of Limit of Detection. The limit of detection for SWV with the fully functionalized electrodes was determined by addition of DNT. The relationship between the maximum current observed at −1750 mV and the concentration of DNT in solution is shown in Figure 10.

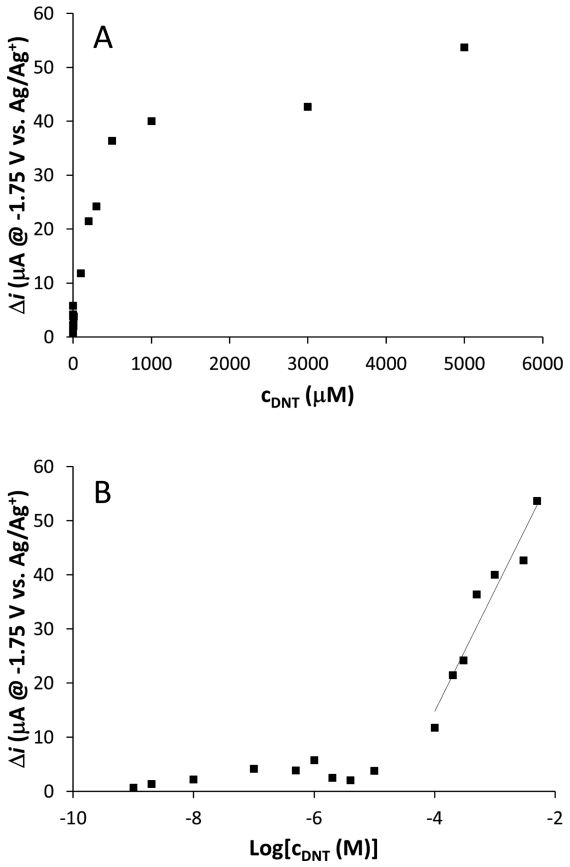

Figure 10. Dependence of the current observed by SWV at −1750 mV on (A) DNT concentration and (B) logarithm of DNT concentration at a functionalized 3DOM carbon electrode in benzotrifluoride/100 mM NBu_4BArF_{24}. T = 20 °C, SW pulse length = 500 ms, SW amplitude = 101 mV, potential step =5 mV.

Inspection of the relationship between peak current and concentration observed in Figure 10 reveals that DNT may be adsorbed onto the surface of 3DOM carbon prior to detection. As shown in Figure 10B, there is a linear relationship between the peak current and the logarithm of the DNT concentration above 1×10^{-4} M. This strongly suggests that adsorbed DNT is indeed being detected by SWV, as expected. A detection limit of 10 μM was obtained, which is comparable to a previously published detection limit of 5 μM for TNT in acetonitrile by SWV with a glassy carbon electrode.[16] Moreover, with an unfunctionalized 3DOM carbon electrode no signal was observed for DNT by SWV at concentrations below 200 μM (see Figure S3 in the Supporting Information). The poor limit of detection for the unmodified electrode indicates a rather large preconcentration of DNT at the surface of the modified electrodes, resulting from the interaction of DNT with the receptors that have been linked to the electrode surface.

Lastly, SWV was performed with 1 mM solutions of the electroactive interferent nitrobenzene to determine the limit of detection for DNT in the presence of an electroactive molecule. Because nitrobenzene is electroactive and present in a rather large concentration, the electrode shows a response at −2.0 V for this molecule. However, as shown in Figure S4 in the Supporting Information, the presence of nitrobenzene in the solution does not affect the limit of detection observed for DNT. As before, the shape of the current−concentration relationship in the presence of nitrobenzene strongly suggests that adsorbed DNT is being detected. This indicates that the binding coefficient of the receptor toward DNT is substantially stronger than that for nitrobenzene.

CONCLUSIONS

In this work, the pore walls of 3DOM carbon electrodes were successfully modified with DNT receptors. DNT was detected by cyclic voltammetry, but this requires a high concentration to give even a small peak due to the high surface area, and consequently large interfacial capacitance, of the 3DOM carbon electrode. To overcome this problem, square wave voltammetry was used, resulting in a detection limit of 10 μM for DNT. The concentration dependence of the observed current indicates that receptor-bound DNT is being detected at all but the highest DNT concentrations, where DNT diffusion to the electrode starts to dominate. Moreover, the addition of receptor molecules to the surface of the 3DOM carbon electrodes provides selectivity for DNT over interferents such as nitrobenzene. These receptors were designed to take advantage of the slightly acidic nature of DNT while at the same time including hydrogen bond-donating sites to further stabilize the deprotonated DNT and thus increase the binding affinity for DNT. The application of these receptor-based sensors to real life samples will be able to take advantage of further preconcentration when DNT (which has a relatively high preference for organic phases and a low vapor pressure) partitions between aqueous or gaseous samples and the organic electrolyte solutions used in this work. It remains to be seen to what extent this will lower detection limits of analysis methods based on these receptor-modified electrodes.

ASSOCIATED CONTENT

Supporting Information

Structure of the electrolyte (NBu_4BArF_{24}), detection of DNT in the presence of potential interferents, and response of an unfunctionalized 3DOM carbon electrode in SWV measurements. This material is available free of charge via the Internet at http://pubs.acs.org.

AUTHOR INFORMATION

Corresponding Author

*E-mail: buhlmann@umn.edu (P.B.); a-stein@umn.edu (A.S.). Phone: 612-624-1431 (P.B.); 612-624-1802 (A.S.). Fax: 612-626-7541 (P.B.); 612-626-7541 (A.S.).

Present Address

[†]Department of Chemistry, Hamline University, 1536 Hewitt Avenue, Saint Paul, Minnesota 55104, United States

Notes

The authors declare no competing financial interest.

■ ACKNOWLEDGMENTS

This work was supported by the National Science Foundation (EXP-SA 0730437, OISE CHE-0809328) and the MRSEC program of the NSF (DMR-0212302 and DMR-0819885). M.A.F. thanks the University of Minnesota for a Doctoral Dissertation Fellowship and 3M Fellowship. Portions of this work were carried out in the University of Minnesota Characterization Facility, which receives partial support from the NSF through the MRSEC, ERC, MRI, and NNIN programs.

■ REFERENCES

(1) Yinon, J. *Trends Anal. Chem.* **2002**, *21*, 292−301.
(2) Steinfield, J. I.; Wormhoudt, J. *Annu. Rev. Phys. Chem.* **1998**, *49*, 203−232.
(3) Yinon, J. *Anal. Chem.* **2003**, *75*, 99A−105A.
(4) Moore, D. S. *Rev. Sci. Instrum.* **2004**, *75*, 2499−2512.
(5) Harper, R. J.; Almirall, J. R.; Furton, K. G. *Talanta* **2005**, *67*, 313−327.
(6) Phelan, J. M.; Barnett, J. L. *Proc. SPIE−Int. Soc. Opt. Eng.* **2002**, *4742*, 532−543.
(7) Sohn, H.; Sailor, M. J.; Magde, D.; Trogler, W. C. *J. Am. Chem. Soc.* **2003**, *125*, 3821−3830.
(8) Naddo, T.; Che, Y.; Zhang, W.; Balakrishnan, K.; Yang, X.; Yen, M.; Zhao, J.; Moore, J. S.; Zang, L. *J. Am. Chem. Soc.* **2007**, *129*, 6978−6979.
(9) Eastwood, D.; Fernandez, C.; Yoon, B. Y.; Sheaff, C. N.; Wai, C. M. *Appl. Spectrosc.* **2006**, *60*, 958−963.
(10) Forzani, E. S.; Lu, D.; Leright, M. J.; Aguilar, A. D.; Tsow, F.; Iglesias, R. A.; Zhang, Q.; Lu, J.; Li, J.; Tao, N. *J. Am. Chem. Soc.* **2009**, *131*, 1390−1391.
(11) Rodríguez, M. C.; Monti, M. R.; Argaraña, C. E.; Rivas, G. A. *Talanta* **2006**, *68*, 1671−1676.
(12) Pinnaduwage, L. A.; Thundat, T.; Hawk, J. E.; Hedden, D. L.; Britt, P. F.; Houser, E. J.; Stepnowski, S.; McGill, R. A.; Bubb, D. *Sens. Actuators, B* **2004**, *99*, 223−229.
(13) Albert, K. J.; Myrick, M. L.; Brown, S. B.; James, D. L.; Milanovich, F. P.; Walt, D. R. *Environ. Sci. Technol.* **2001**, *35*, 3193−3200.
(14) Masunaga, K.; Hayama, K.; Onodera, T.; Hayashi, K.; Miura, N.; Matsumoto, K.; Toko, K. *Sens. Actuators, B* **2005**, *108*, 427−434.
(15) Nie, D.; Li, P.; Zhang, D.; Zhou, T.; Liang, Y.; Shi, G. *Electrophoresis* **2010**, *31*, 2981−2988.
(16) Saravanan, N. P.; Venugopalan, S.; Senthilkumar, N.; Santhosh, P.; Kavita, B.; Prabu, H. G. *Talanta* **2006**, *69*, 656−662.
(17) Honeychurch, K. C.; Hart, J. P.; Pritchard, P. R. J.; Hawkins, S. J.; Ratcliffe, N. M. *Biosens. Bioelectron.* **2003**, *19*, 305−312.
(18) Agüí, L.; Vega-Montenegro, D.; Yáñez-Sedeño, P.; Pingarrón, J. M. *Anal. Bioanal. Chem.* **2005**, *382*, 381−387.
(19) Huang, M.-J.; Leszczynski, J. *J. Mol. Struct.−Theochem.* **2002**, *592*, 105−113.
(20) Lehn, J.-M. *Supramolecular Chemistry: Concepts and Perspectives*; Wiley-VCH: Weinheim, Germany, 1995.
(21) Yang, X.; Du, X.-X.; Shi, J.; Swanson, B. *Talanta* **2001**, *54*, 439−445.
(22) Shankaran, D. R.; Kawaguchi, T.; Kim, S. J.; Matsumoto, K.; Toko, K.; Miura, N. *Anal. Bioanal. Chem.* **2006**, *108*, 1313−1320.
(23) Walcarius, A. *Anal. Bioanal. Chem.* **2010**, *396*, 261−272.
(24) Walcarius, A. *Trends Anal. Chem.* **2012**, *38*, 79−97.
(25) Ergang, N. S.; Fierke, M. A.; Wang, Z.; Smyrl, W. H.; Stein, A. *J. Electrochem. Soc.* **2007**, *154*, A1135−A1139.
(26) Wang, Z.; Fierke, M. A.; Stein, A. *J. Electrochem. Soc.* **2008**, *155*, A658−A663.
(27) Fierke, M. A.; Lai, C.-Z.; Bühlmann, P.; Stein, A. *Anal. Chem.* **2010**, *82*, 680−688.
(28) Lai, C.-Z.; Fierke, M. A.; Stein, A.; Bühlmann, P. *Anal. Chem.* **2007**, *79*, 4621−4626.
(29) Lai, C.-Z.; Joyer, M. M.; Fierke, M. A.; Petkovich, N. D.; Stein, A.; Bühlmann, P. *J. Solid State Electrochem.* **2009**, *13*, 123−128.
(30) Zhang, T.; Lai, C.-Z.; Fierke, M. A.; Stein, A.; Bühlmann, P. *Anal. Chem.*, in press, dx.doi.org/10.1021/ac3011507.
(31) Bühlmann, P.; Nishizawa, S.; Xiao, K. P.; Umezawa, Y. *Tetrahedron* **1997**, *53*, 1647−1654.
(32) Olson, E. J.; Xiong, T. T.; Cramer, C. J.; Bühlmann, P. *J. Am. Chem. Soc.* **2011**, *133*, 12858−12865.
(33) Delamar, M.; Hitmi, R.; Pinson, J.; Savéant, J.-M. *J. Am. Chem. Soc.* **1992**, *114*, 5883−5884.
(34) Allongue, P.; Delamar, M.; Desbat, B.; Fagebaume, O.; Hitmi, R.; Pinson, J.; Savéant, J.-M. *J. Am. Chem. Soc.* **1997**, *119*, 201−207.
(35) Boswell, P. G.; Bühlmann, P. *J. Am. Chem. Soc.* **2005**, *127*, 8958−8959.
(36) Nishida, H.; Takada, N.; Yoshimura, M.; Sonoda, T.; Kobayashi, H. *Bull. Chem. Soc. Jpn.* **1984**, *57*, 2600−2604.
(37) Yakelis, N. A.; Bergman, R. G. *Organometallics* **2005**, *24*, 3579−3581.
(38) Hill, M. G.; Lamanna, W. M.; Mann, K. R. *Inorg. Chem.* **1991**, *30*, 4687−4690.
(39) Saby, C.; Ortiz, B.; Champagne, G. Y.; Bélanger, D. *Langmuir* **1997**, *13*, 6805−6813.
(40) Liu, Y.-C.; McCreery, R. L. *J. Am. Chem. Soc.* **1995**, *117*, 11254−11259.
(41) Yu, S. S. C.; Tan, E. S. Q.; Jane, R. T.; Downard, A. J. *Langmuir* **2007**, *23*, 11074−11082.
(42) Hurley, B. L.; McCreery, R. L. *J. Electrochem. Soc.* **2004**, *151*, B252−B259.
(43) D'Amours, M.; Bélanger, D. *J. Phys. Chem. B* **2003**, *107*, 4811−4817.
(44) Doppelt, P.; Hallais, G.; Pinson, J.; Podvorica, F.; Verneyre, S. *Chem. Mater.* **2007**, *19*, 4570−4575.
(45) Brooksby, P. A.; Downard, A. J. *J. Phys. Chem. B* **2005**, *109*, 8791−8798.
(46) Ortiz, B.; Saby, C.; Champagne, G. Y.; Bélanger, D. *J. Electroanal. Chem.* **1998**, *455*, 75−81.
(47) Boehm, H. P. In *Graphite and Precursors*; Delhaes, P., Ed.; Gordon and Breach Science Publishers: Amsterdam, The Netherlands, 2001; Vol. *1*, pp 141−178.
(48) Prest, J. W. M.; Mosher, R. A. In *Colloids and Surfaces in Reprographic Technology*; Hair, M., Croucher, M. D., Eds.; American Chemical Society: Washington, D.C., 1982; pp 225−247.
(49) Liu, L.; Qin, Y.; Guo, Z.-X.; Zhu, D. *Carbon* **2003**, *41*, 331−335.
(50) Sainsbury, T.; Fitzmaurice, D. *Chem. Mater.* **2004**, *16*, 3780−3790.
(51) Shaffer, M. S. P.; Fan, X.; Windle, A. H. *Carbon* **1998**, *36*, 1603−1612.
(52) Pretsch, E.; Bühlmann, P.; Badertscher, M. *Structure Determination of Organic Compounds: Tables of Spectral Data*, 4th ed.; Springer: Berlin, 2009.
(53) Silverstein, R. M.; Webster, F. X. *Spectrometric Identification of Organic Compounds*, 6th ed.; John Wiley & Sons: Hoboken, NJ, 1998.
(54) Krausa, M.; Doll, J.; Schorb, K.; Böke, W.; Hambitzer, G. *Propellants, Explos., Pyrotech.* **1997**, *22*, 156−159.
(55) Zhang, H.-X.; Zhang, J.-H. *Can. J. Chem.* **2011**, *89*, 8−12.
(56) Zang, J.; Guo, C. X.; Hu, F.; Yu, L.; Li, C. M. *Anal. Chim. Acta* **2011**, *683*, 187−191.
(57) Zhang, H.-X.; Cao, A.-M.; Hu, J.-S.; Wan, L.-J.; Lee, S.-T. *Anal. Chem.* **2006**, *78*, 1967−1971.
(58) Fry, A. J. *J. Electroanal. Chem.* **2003**, *546*, 35−39.
(59) Helfrick, J. J. C.; Bottomley, L. A. *Anal. Chem.* **2009**, *81*, 9041−9047.
(60) Bard, A. J.; Faulkner, L. R. *Electrochemical Methods: Fundamentals and Applications*, 2nd ed.; Wiley: New York, 2001.
(61) O'Dea, J. J.; Osteryoung, J.; Lane, T. *J. Phys. Chem.* **1986**, *90*, 2761−2764.
(62) O'Dea, J. J.; Osteryoung, J.; Osteryoung, R. A. *J. Phys. Chem.* **1983**, *87*, 3911−3918.

(63) O'Dea, J. J.; Osteryoung, J.; Osteryoung, R. A. *Anal. Chem.* **1981**, *53*, 695−701.
(64) O'Dea, J. J.; Wikiel, K.; Osteryoung, J. *J. Phys. Chem.* **1990**, *94*, 3628−3636.
(65) Chuang, M.-C.; Windmiller, J. R.; Santhosh, P.; Ramírez, G. V.; Galik, M.; Chou, T.-Y.; Wang, J. *Electroanalysis* **2010**, *22*, 2511−2518.
(66) Bozic, R. G.; West, A. C.; Levicky, R. *Sens. Actuators, B* **2008**, *133*, 509−515.
(67) Osteryoung, J. G.; Osteryoung, R. A. *Anal. Chem.* **1985**, *57*, 101A−110A.